Electronic Supplementary Material (ESI) for RSC Advances.

Sodium ion intercalation and multi redox behavior of keggin type polyoxometalate during $[PMo_{10}V_2O_{40}]^{5-}$ to $[PMo_{10}V_2O_{40}]^{27-}$ as cathode material for Na-ion rechargeable batteries

Marimuthu Priyadarshini[1], Swaminathan Shanmugan[1*], Kiran Preethi Kirubakaran[1,2], Anoopa Thomas[1], Muthuramalingam Prakash[1]and Kumaran Vediappan[1*]

[1]Department of Chemistry, Faculty of Engineering and Technology, SRM Institute of Science and Technology, Kattankulathur-603203, Tamil Nadu, India

[2]Department of Physics and Nanotechnology, Faculty of Engineering and Technology, SRM Institute of Science and Technology, Kattankulathur-603203, Chennai, Tamil Nadu, India

Methods

The crystallinity and the phase purity of the samples were studied by Powdered X-ray diffraction (PXRD, PANalytical India, Spectris Technologies) with Cu Ka radiation (λ= 1.54 Å). To analyze the nature of bonding between the metals and oxygen, Fourier transform infrared (FT-IR, Shimadzu IR Tracer-100) was used. Thermogravimetric analysis (TGA) at a heating rate of 10 ^{o}C min^{-1} was analyzed to find out the amount of weight loss and the stability of the materials using Netzsch STA 2500 Regulus. The morphologies and the particle size of the samples were studied from Field Emission-Scanning Electron Microscope (FE-SEM, FEI QUANTA 200) and using High Resolution-Transmission Electron Microscope (HR-TEM, Jeol-JEM 2100 Plus). To confirm the elemental composition X-ray photoelectron spectroscopy (XPS) was carried out on a ULVAC-PHI, PHI5000 Version Probe III, Physical Electronics equipment. Cyclic Voltammetry (CV) is performed in scan rates 0.1, 0.25, 0.50, 1.0 V between 2.0 – 4.5 V voltage ranges and Electrochemical Impedance Spectroscopy (EIS) were measured on Biologic Electrochemical workstation (BioLogic–SAS, VSP-300). Galvanostatic charge-discharge tests were measured on Neware battery cycler (versus Na^{+}/Na).

Computational Methods

Here, we explored the structures of POM^{5-} and POM^{27-} using DFT-PBE based periodic calculations. Also, the structure and properties of the $Na_5[PMo_{10}V_2O_{40}]$ cluster is analyzed using same methodology and compared with our previous report[1]. The Keggin-type structure of POM was obtained from the available experimental crystal structure[2]. In our previous work, we reported that the ions such as H^{+}, Li^{+} can stabilize at the inter-cluster space between the POM clusters[1]. Similarly, in present study we considered five Na^{+} cations which are placed near to the POM and freely optimized, without any constraints. The optimized geometry is further used for

the analysis of structural changes in the interstitial sites, adsorption energy of metal ions and to quantify the characteristic charge transfer between Na and POM. Furthermore to analyze the discharged state of POM, we incorporated 27 Na^+ ions surrounding the POM cluster, so that the resulting structure is POM^{27-}. These two structures (POM^{5-} and POM^{27-}) represent the charged and discharged states of POM, respectively. All the DFT periodic calculations are carried out using PBE (Perdew-Burke-Ernzerhof)[3] method with Grimme's D3[4] dispersion correction (PBE-D3). This method can accurately predict the properties of many inorganic clusters and energy storage materials[1,5]. The CP2K CELLOPT protocol was used to optimize the geometries to understand the structural changes happening to the cluster during the charge/discharge states. All the calculations are carried out using Quickstep package of CP2K 5.1[6]. The DZVP (double zeta valence polarized) basis set is used for all the atoms, except for oxygen. For oxygen atoms we used TZVP (triple zeta valence polarized) basis set[7]. The Gaussian plane wave (GPW)[8] is used for the description of pseudopotentials and valence electron density of the system. Orbital transformation (OT)[9] and plane wave cut-off (400 Ry) was also incorporated. The GTH (Goedecker-Teter-Hutter)[10] pseudopotentials are used for all the elements. The computational protocol was followed as per our previous work for the comparison of different clusters[1]. Due to computational constraints, the partially optimized structure of super-reduced POM was considered for comparison with the reduced state. After optimization, the geometry, binding energy (BE) and Lowdin charge transfer between cations and anionic cluster are analyzed for understanding the electronic behavior of the system. The BE is calculated as follows,

$$BE = E_{total} - (E_{cation} + E_{anion})$$

where E_{total} is the total energy of the POM with Na cations, E_{cation} is the energy of 5 Na^+ cations and E_{anion} is the energy of anionic part of the structure.

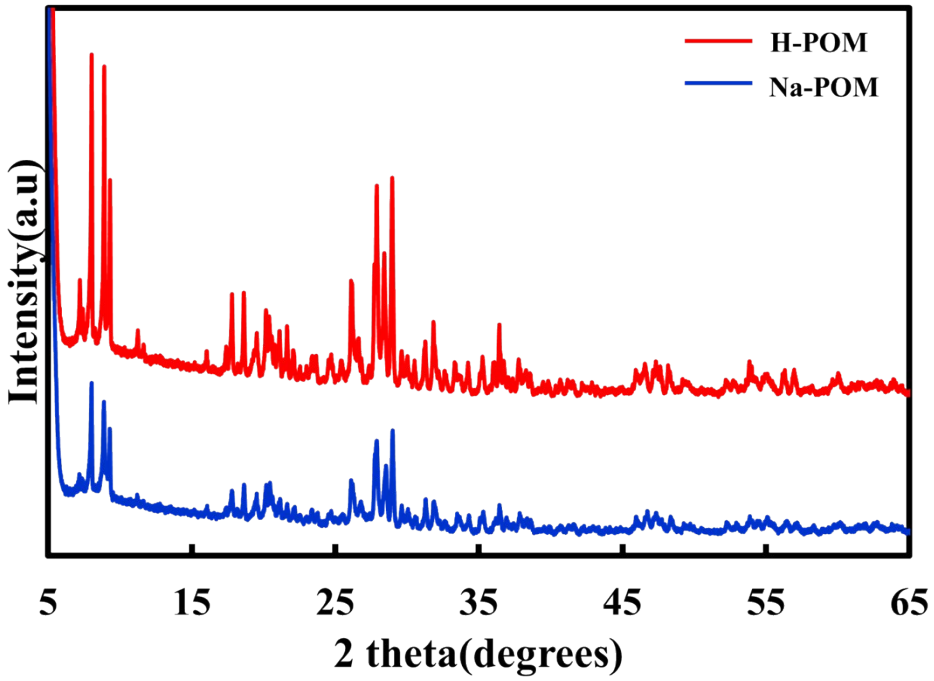

Fig. S1 XRD plots of H-POM and Na-POM

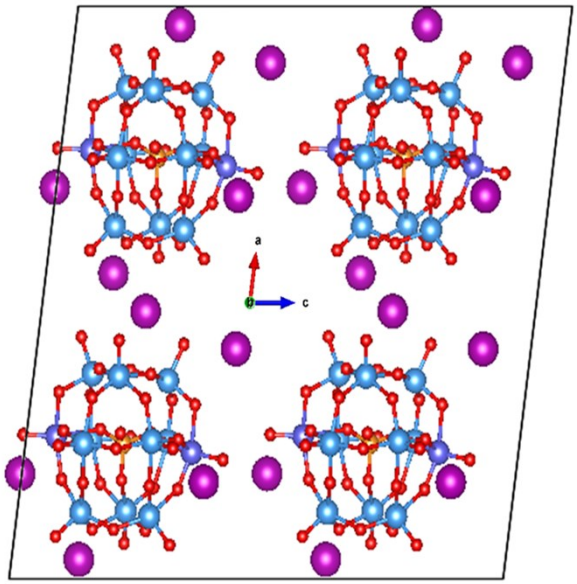

Fig. S2 Optimized geometry of $Na_5[PMo_{10}V_2O_{40}]$ complex a 2x2x2 super cell of Na-POM

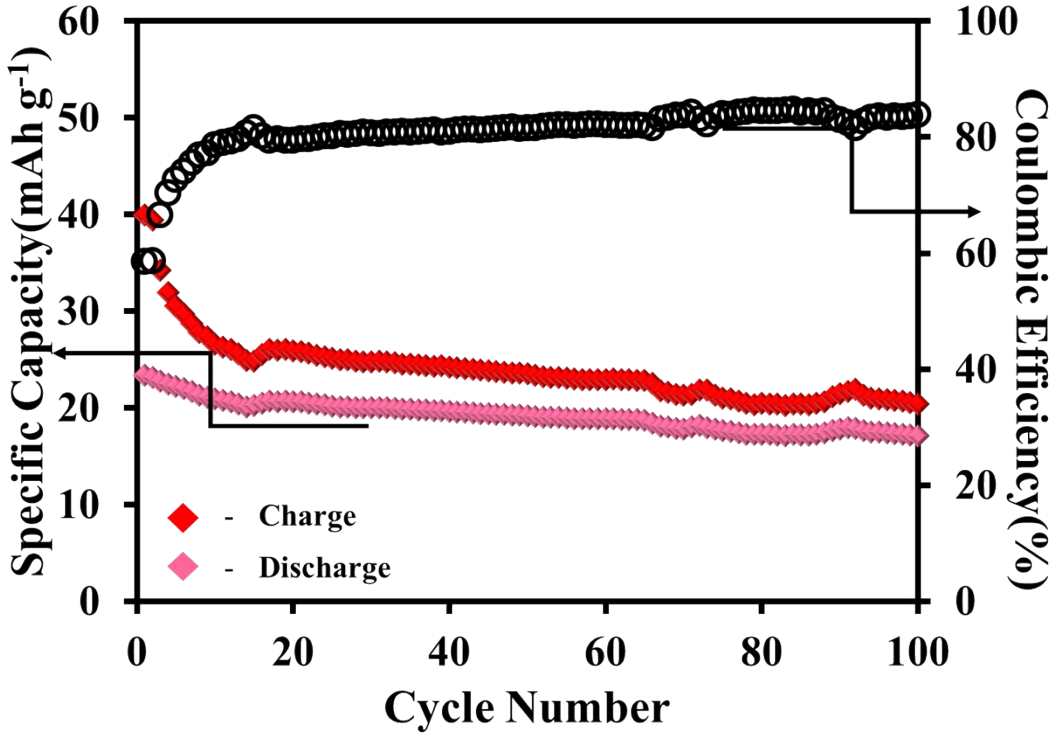

Fig. S3 Life cycle performance of H-POM at 0.1C for 100 cycle

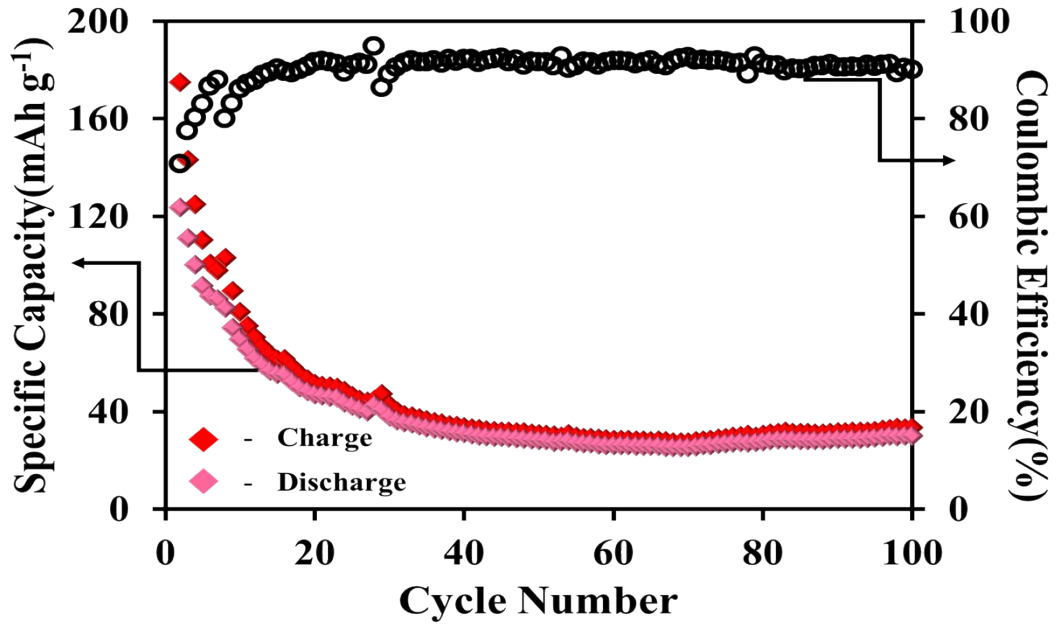

Fig. S4 Life cycle performance of Na-POM at 0.1C for 100 cycle

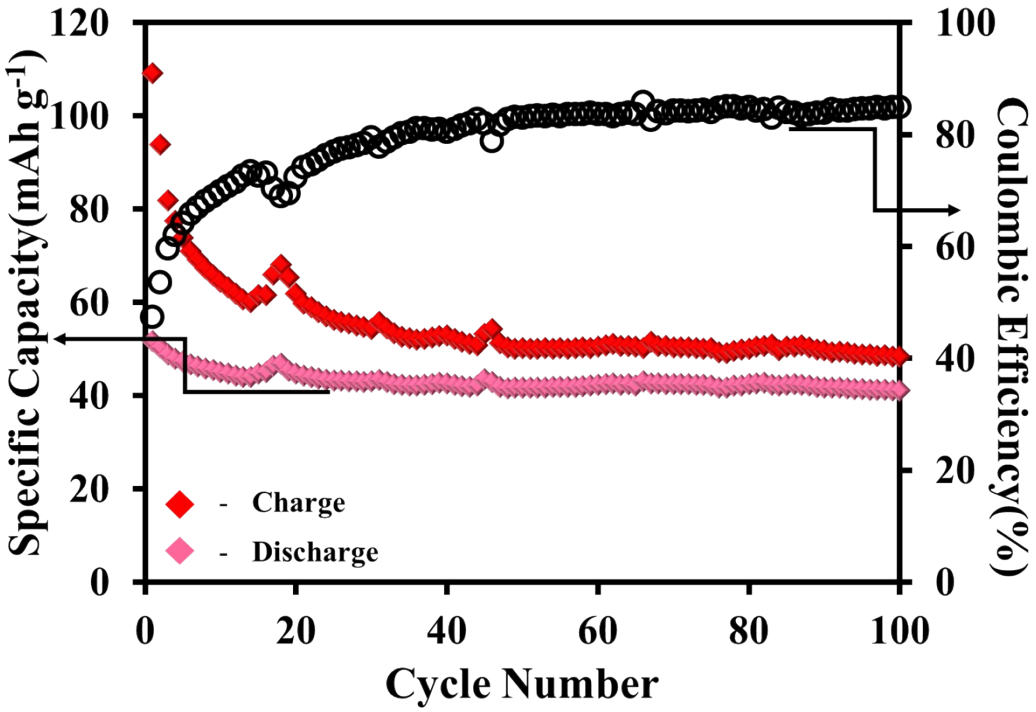

Fig. S5 Life cycle performance of Na-POM at 1C for 100 cycle.

Table. S1 The calculated structural parameters, adsorption energy and charge transfer for optimized $Na_5[PMo_{10}V_2O_{40}]$ the respective units were provided in parenthesis

$Na_5[PMo_{10}V_2O_{40}]$	
a (Å)	11.52
b (Å)	11.66
c (Å)	11.24
α (°)	87.67
β (°)	82.45
γ (°)	97.68
E_{ads}(in eV)	-32.91
Volume change (%)	36.003
Charge transfer (a.u)	-3.63/3.63 (anion/cation)

Table. S2 Table comparing the electrochemical properties of POM as electrode for Na-ion batteries

Electrode Material	Polyoxometalate type	Type	C rate/ Current density	Electrode composition (SM:CB:B)	No of cycles	Specific Capacity (mAh/g)	Ref.
$Na_2H_8[MnV_{13}O_{38}]$	-	Cathode	0.1 C	70:20:10	100	190	[11]
$Li_7[V_{15}O_{36}(CO_3)]$	-	Cathode	100 mAg^{-1}	70:20:10	30	190	[12]
$Na_6[V_{10}O_{28}]\cdot 16H_2O$	Decavanadate	Anode	20 mAg^{-1}	60:20:20	100	276	[13]
$Na_5PMo_{10}V_2O_{40}$	Keggin	Cathode	0.1 C	50:40:10	100	123	This Work

References

1 M. Priyadarshini, S. Shanmugan, K. P. Kirubakaran, A. Thomas, M. Prakash, C. Senthil, C. W. Lee and K. Vediappan, *J. Phys. Chem. Solids*, 2020, **142**, 109468.

2 M. I. Khan, S. Cevik and R. Hayashi, *Dalt. Trans.*, 1999, 1651–1654.

3 J. P. Perdew, K. Burke and M. Ernzerhof, *Phys. Rev. Lett.*, 1996, **77**, 3865.

4 J. C. Phys, S. Grimme, J. Antony, S. Ehrlich and H. Krieg, *J. Chem. Phys.*, 2016, **132**, 154104–15123.

5 K. P. Kirubakaran, C. Senthil, M. Priyadarshini, S. Kamalakannan, M. Prakash, V. Vinesh, B. Neppolian, V. Ganesh, C. W. Lee and K. Vediappan, *Energy Storage*, , DOI:10.1002/est2.133.

6 J. Vandevondele, M. Krack, F. Mohamed, M. Parrinello, T. Chassaing and J. Hutter, *Comput. Phys. Commun.*, 2005, **167**, 103–128.

7 J. VandeVondele and J. Hutter, *J. Chem. Phys.*, 2007, **127**, 114105.

8 G. Lippert, J. Hutter and M. Parrinello, *Theor. Chem. Acc.*, 1999, **103**, 124–140.

9 J. VandeVondele and J. Hutter, *J. Chem. Phys.*, 2003, **118**, 4365–4369.

10 S. Goedecker, M. Teter and J. Hutter, *Phys. Rev. B*, 1996, **54**, 1703.

11 J. Liu, Z. Chen, S. Chen, B. Zhang, J. Wang, H. Wang, B. Tian, M. Chen, X. Fan, Y. Huang, T. C. Sum, J. Lin and Z. X. Shen, *ACS Nano*, 2017, **11**, 6911–6920.

12 J. J. Chen, J. C. Ye, X. G. Zhang, M. D. Symes, S. C. Fan, D. L. Long, M. Sen Zheng, D. Y. Wu, L. Cronin and Q. F. Dong, *Adv. Energy Mater.*, 2018, **8**, 1–6.

13 S. Hartung, N. Bucher, H. Y. Chen, R. Al-Oweini, S. Sreejith, P. Borah, Z. Yanli, U. Kortz, U. Stimming, H. E. Hoster and M. Srinivasan, *J. Power Sources*, 2015, **288**, 270–277.